Discretization of Linear Fractional Representations of LPV systems

R. Tóth, M. Lovera, P. S. C. Heuberger and P. M. J. Van den Hof

***Abstract*— Commonly, controllers for Linear Parameter-Varying (LPV) systems are designed in continuous-time using a Linear Fractional Representation (LFR) of the plant. However, the resulting controllers are implemented on digital hardware. Furthermore, discrete-time LPV synthesis approaches require discrete-time model of the plant which is often derived from continuous-time first-principle models. Existing discretization approaches of LFRs suffer from disadvantages like alternation of dynamics, complexity, etc. To overcome the disadvantages, novel discretization methods are derived. These approaches are compared to existing techniques and analyzed in terms of approximation error, considering ideal zero-order hold actuation and sampling.**

***Index Terms*— Linear fractional representation, discretization**

I. INTRODUCTION

Control synthesis approaches for *Linear Parameter-Varying* (LPV) systems (like [1], [2], [3]), often require LPV models of the plant in a *Linear Fractional Representation* (LFR), as depicted in Figure 1a. In the LPV interpretation of LFRs, the feedback gain Δ is assumed to vary in time as Δ is a function of a measurable signal, the so-called scheduling variable $p : \mathbb{R} \rightarrow \mathbb{P}$. The compact set (or polytope) $\mathbb{P} \subseteq \mathbb{R}^{n_\mathbb{P}}$ denotes the scheduling space. Using scheduling variables as changing operating conditions or endogenous/free signals of the plant, LPV representations can describe both nonlinear and time-varying phenomena.

In practice, implementation of LPV control designs in physical hardware often meets significant difficulties, as mostly *continuous-time* (CT) LPV controllers [1], [2] are preferred in the literature over *discrete-time* (DT) solutions [4], [5]. The main reason is that stability and performance requirements can be more conveniently expressed in CT, like in a mixed sensitivity setting [3]. Therefore, the current design tools focus on continuous-time LPV controller synthesis in an LFR form, requiring efficient discretization of such system representations for implementation purposes. Next to that, DT approaches require a DT model of the plant which is often available only through the use of CT first-principle models. It follows that discretization of LFRs is a crucial issue for both control design and controller implementation.

In the existing literature, some approaches of LFR discretization are available. However, the validity of the used discretization settings or the introduced approximation error has not been analyzed so far. Basically the available methods use *Zero-Order Hold* (ZOH) and *First-Order Hold* (1OH) approaches to restrict the variations of the signals of the LFR in the sample interval which results in a DT description of the dynamics [6], [7], [8], [9], [10], [11], [12], [13]. Almost all of these methods suffer from various disadvantages like significant approximation errors, loss of stability, high complexity etc., see Section III.

In this paper, we aim to give an analysis of discretization settings in the LFR case and to derive exact extensions of the approaches of the LTI framework. We intend to develop reliable and easy to use LFR discretization methods. We also compare the properties of the resulting approaches in terms of preservation of stability, and discretization errors.

The paper is organized as follows: First, in Section II, LFRs of LPV systems are defined. In Section III existing approaches of LFR discretization are investigated pointing out the need for improvement. Using an exact discretization setting in Section IV, popular discretization methods of the LTI framework are extended to LFRs. In Section V, properties of the introduced methods are presented in terms of discretization error and preservation of stability. In Section VI, a numerical example is given for the comparison of the approaches. Finally in Section VII, the main conclusions of the paper are drawn.

II. LINEAR FRACTIONAL REPRESENTATIONS

First, LFRs are defined in CT and DT. For a given continuous-time LPV system $\mathcal{S}$, the LFR of $\mathcal{S}$, denoted by $\mathfrak{R}_{\mathrm{LFR}}(\mathcal{S})$, is defined as

$$\begin{bmatrix} \dot{x}(t) \\ z(t) \\ y(t) \end{bmatrix} = \begin{bmatrix} A & B_1 & B_2 \\ C_1 & D_{11} & D_{12} \\ C_2 & D_{21} & D_{22} \end{bmatrix} \begin{bmatrix} x(t) \\ w(t) \\ u(t) \end{bmatrix} \qquad (1a)$$

where $u : \mathbb{R} \rightarrow \mathbb{U} = \mathbb{R}^{n_\mathbb{U}}$ and $y : \mathbb{R} \rightarrow \mathbb{Y} = \mathbb{R}^{n_\mathbb{Y}}$ are the input and output signals of the system $\mathcal{S}$, containing disturbance/actuated input and measurable/unmeasurable output channels alike. $x : \mathbb{R} \rightarrow \mathbb{X} = \mathbb{R}^{n_\mathbb{X}}$ is the state variable of the representation. $\{A, \ldots, D_{22}\}$ are constant matrices with appropriate dimensions and

$$w(t) = \Delta(p(t))z(t), \qquad (1b)$$

where $\Delta : \mathbb{P} \rightarrow \mathbb{R}^{n_\mathrm{P} \times n_\mathrm{P}}$ is a function of the scheduling signal p of $\mathcal{S}$. Commonly, Δ has a block diagonal structure containing the elements of p and Δ is assumed to vary in a polytope. Note that (1a-b) is a *Differential Algebraic Equation* (DAE), instead of an *Ordinary Differential Equation* (ODE) encountered in state-space representations. Additionally, x, w, z are latent (auxiliary) variables of $\mathfrak{R}_{\mathrm{LFR}}(\mathcal{S})$.

R. Tóth, P. S. C. Heuberger and P. M. J. Van den Hof are with the Delft Center for Systems and Control, Delft University of Technology, Mekelweg 2, 2628 CD, Delft, The Netherlands, email: {r.toth,p.s.c.heuberger,p.m.j.vandenhof}@tudelft.nl.

M. Lovera is with the Dipartimento di Elettronica e Informazione, Politecnico di Milano, Piazza Leonardo da Vinci 20133, Milano, Italy, email: lovera@elet.polimi.it.

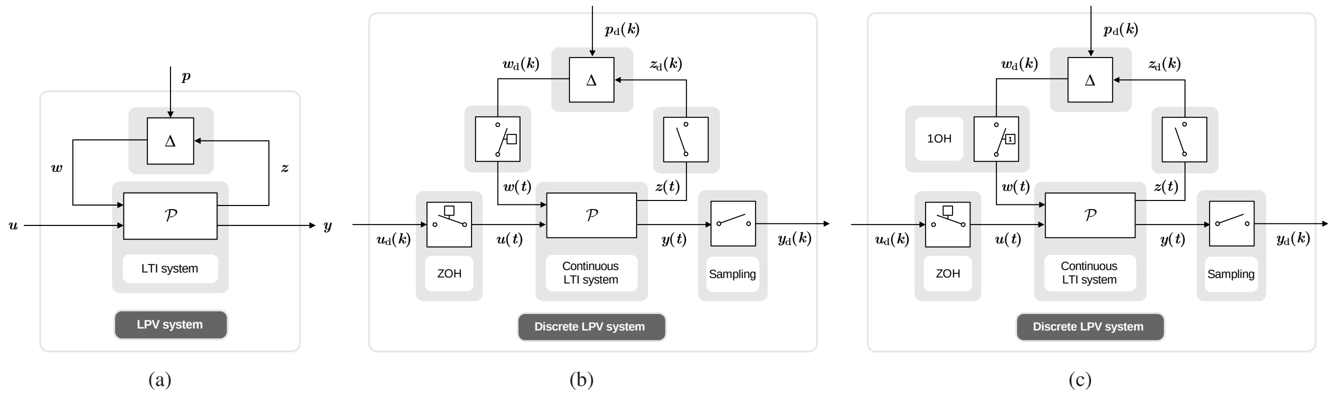

Fig. 1. (a) Linear fractional representation of LPV systems. (b) Full ZOH discretization of LFRs. (c) First/Zero-order hold discretization of LFRs.

By defining y_d, u_d, p_d as the sampled signals of y, u, p with *sampling time* $\mathtt{T}_\mathrm{d} > 0$, e.g. $u_\mathrm{d}(k) := u(k\mathtt{T}_\mathrm{d})$, the definition of a LFR can be established in DT as the representation of an underlying sampled continuous-time LPV system $\mathcal{S}$:

$$\begin{bmatrix} x_\mathrm{d}(k+1) \\ z_\mathrm{d}(k) \\ y_\mathrm{d}(k) \end{bmatrix} = \begin{bmatrix} \Phi & \Gamma_1 & \Gamma_2 \\ \Upsilon_1 & \Omega_{11} & \Omega_{12} \\ \Upsilon_2 & \Omega_{21} & \Omega_{22} \end{bmatrix} \begin{bmatrix} x_\mathrm{d}(k) \\ w_\mathrm{d}(k) \\ u_\mathrm{d}(k) \end{bmatrix} \quad (2)$$

where $\{\Phi, \ldots, \Omega_{22}\}$ are constant matrices with appropriate dimensions and $w_\mathrm{d}(k) = \Delta_\mathrm{d}(p_\mathrm{d}(k))z_\mathrm{d}(k)$ with $\Delta_\mathrm{d} : \mathbb{P} \to \mathbb{R}^{n_\mathrm{p} \times n_\mathrm{p}}$. Note that it is not necessary that z_d, w_d, or x_d are also sampled signals of their CT counterparts (they are just latent variables). In the sequel, this representation is denoted as $\mathfrak{R}_\mathrm{LFR}(\mathcal{S}, \mathtt{T}_\mathrm{d})$. Now we can define the problem we intend to focus in the rest of the paper:

Problem 1 (Discretization problem): For a sampling time $\mathtt{T}_\mathrm{d} > 0$ and for a given LFR of a CT-LPV system $\mathcal{S}$, find a DT-LFR that describes or approximates the sampled behavior of the output signal y of $\mathcal{S}$ for all possible trajectories of the input u and the scheduling variable p. □

III. Existing discretization approaches

Before deriving a solution to Problem 1, the existing LFR discretization approaches are investigated by evaluating their performance in terms of the proposed problem setting and also pointing out the need for improvements.

A. Basic concepts of the discretization settings

In the available literature, only the isolated setting (stand alone discretization of the system) is treated where some signals of the CT-LFR are restricted in variation during a fixed sampling interval while other signals are sampled.

The simplest case is when a *Zero-Order-Hold* (ZOH) is applied on a set of signals restricting their variation to be piecewise-constant. Similar to the LTI case, it is necessary to restrict the free variables of the system, i.e. u and p, to be piece-wise constant, piece-wise linear (called *first-order-hold*), or 2^nd-order polynomial (called *second-order-hold*), etc. in order to describe the evolution of all non-free variables inside the sampling interval. This makes it possible to derive a DT description of the system where signals are only observed at the sampling time instants. In order to simplify the discretization problem the following assumption is commonly used:

Assumption 1 (Discretization setting): The hold and the sampling devices are perfectly synchronized with $\mathtt{T}_\mathrm{d} > 0$ as the *sampling time* or *discretization time-step*. Furthermore, these devices have infinite resolution (no quantization error) and their processing time is zero. □

Note that due to the assumed ideal hold devices, at the beginning of each sample interval a switching effect occurs. Contrary to the LTI case, the switching effect on p introduces additional dynamics into the system which hardly occurs in reality. Thus to avoid the overcomplicated analysis of such effects the following assumption is made:

Assumption 2 (Switching effects): The switching behavior of the hold devices has no effect on the CT plant, i.e. the switching of the signals is assumed to take place smoothly.

B. Full zero-order hold approaches

A commonly used approach, like in [6], [7], is to apply ZOHs and sampling on all signals of (1a-b) (see Figure 1b). It becomes apparent that this setting implies that (1a) is discretized as a stand-alone (open-loop) LTI system disregarding (1b). The advantage of this method lays in its simplicity, however it can seriously alter the dynamics, i.e. stability, of the DT approximation as it kills all variations of the state that are coupled with Δ.

C. First/Zero-order hold approaches

Other methods, like [8], [9], use a mixed discretization setting of first and zero-order holds depicted in Figure 1c. By considering future samples of p and z in terms of the 1OH, the approximation of the variations of x that are coupled with Δ improves. However, this also turns out to be a disadvantage, as the resulting DT-LFR becomes dependent on future samples of p and w, which results in a non-causal representation.

D. Bilinear transformation technique

As an alternative, the time operator can be extracted as an integrator (see Figure 2a) which is discretized via the z-substitution of its Laplace transform $1/s$ (see [10], [11]). For the substitution, the bilinear transformation

$$\frac{1}{s} \approx \frac{\mathtt{T}_\mathrm{d}}{2}\frac{z+1}{z-1}, \quad (3)$$

is used, resulting in a Tustin type of discretization approach. It can be shown that this intuitive method introduces ZOH only on u and p, depicted in Figure 2b, and it does not restrict variations of the state. Furthermore, this concept preserves stability of the original representation. On the other hand, the formulation of the approach is rather intuitive as it does not give an understanding of the introduced approximations.

E. Discretization in state-space form

Another discretization approach is to rewrite the LFR (1a-b) into an LPV *State-Space* (SS) representation:

$$\dot{x} = \mathcal{A}(p)x + \mathcal{B}(p)u, \tag{4a}$$
$$y = \mathcal{C}(p)x + \mathcal{D}(p)u, \tag{4b}$$

if the following assumption is satisfied:

Assumption 3: $I - D_{11}\Delta(\mathrm{p})$ is invertible for all $\mathrm{p} \in \mathbb{P}$. □

In (4a-b) the matrices are given as

$$\mathcal{A}(p) = A + B_1\Delta(p)(I - D_{11}\Delta(p))^{-1}C_1, \tag{5a}$$
$$\mathcal{B}(p) = B_2 + B_1\Delta(p)(I - D_{11}\Delta(p))^{-1}D_{12}, \tag{5b}$$
$$\mathcal{C}(p) = C_2 + D_{21}\Delta(p)(I - D_{11}\Delta(p))^{-1}C_1, \tag{5c}$$
$$\mathcal{D}(p) = D_{22} + D_{21}\Delta(p)(I - D_{11}\Delta(p))^{-1}D_{12}. \tag{5d}$$

As a next step, the discretization formulas of LPV-SS representations derived in [12], [13] are applied on (4a-b). Then, the resulting discrete-time LPV-SS representation is transformed to a discrete-time LFR. An advantage of this approach is that it provides a wide range of fully analyzed methods with criteria to choose the sampling time. However, conversion between the LFR and SS representations is complicated and the resulting DT-SS representations might not be realizable by an LFR without introducing conservatism (see Section IV-A).

IV. Exact ZOH discretization of LFRs

As we have seen, many existing approaches suffer from various disadvantages, due to the effect of hold devices on the loop (1b). This makes the setting of Figure 2b attractive for discretization, which is also proved by the properties of the associated bilinear method. As this method is only approximative, the question rises whether we can do more in this setting to give a solution to Problem 1. This is investigated in the following part, by using the exact ZOH setting presented in Figure 2b, in order to derive effective discretization approaches of LFRs which overcome the disadvantages of the existing methods.

Using the concept of Figure 2b, the following assumption is introduced:

Assumption 4 (exact ZOH setting): We are given a CT-LPV system $\mathcal{S}$, with CT input signal u, scheduling signal p, and output signal y, where u and p are generated by an ideal ZOH device and y is sampled. Additionally, the ZOHs and the sampling satisfies Assumptions 1-2 with $\mathrm{T_d} > 0$. □

These assumptions imply that

$$u(t) := u_\mathrm{d}(k), \quad \forall t \in [k\mathrm{T_d}, (k+1)\mathrm{T_d}), \tag{6a}$$
$$p(t) := p_\mathrm{d}(k), \quad \forall t \in [k\mathrm{T_d}, (k+1)\mathrm{T_d}), \tag{6b}$$
$$y_\mathrm{d}(k) := y(k\mathrm{T_d}), \tag{6c}$$

for each $k \in \mathbb{Z}$, meaning that u and p can only change at every sampling time instant.

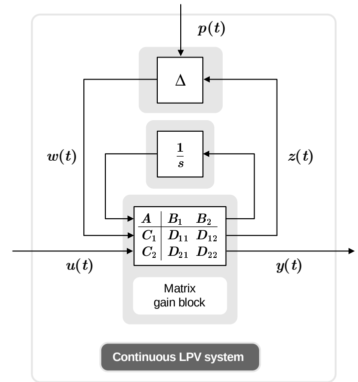

(a)

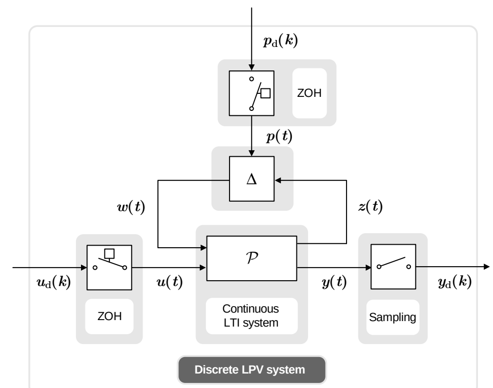

(b)

Fig. 2. (a) Extraction of the integrator for bilinear discretization. (b) Exact ZOH discretization of LFRs.

A. Complete approach

First the complete signal evolution approach [14] of the LTI framework is extended to the LFR case. Let a CT-LFR be given in the ZOH setting of Figure 2b. Based on Assumption 4, i.e. p and u are constant signals inside each sampling interval, (1a) can be written as

$$\begin{bmatrix} \dot{x}(t) \\ z(t) \\ y(t) \end{bmatrix} = \begin{bmatrix} A & B_1\Delta(p(k\mathrm{T_d})) & B_2 \\ C_1 & D_{11}\Delta(p(k\mathrm{T_d})) & D_{12} \\ C_2 & D_{21}\Delta(p(k\mathrm{T_d})) & D_{22} \end{bmatrix} \begin{bmatrix} x(t) \\ z(t) \\ u(k\mathrm{T_d}) \end{bmatrix} \tag{7}$$

which corresponds to a DAE. Now in the k^{th} sampling interval, the state evolution $x(t)$ reads as

$$x(k\mathrm{T_d}) + \int_{k\mathrm{T_d}}^{t} Ax(\tau) + B_1\Delta(p(k\mathrm{T_d}))z(\tau) + Bu(k\mathrm{T_d})d\tau, \tag{8}$$

where $z(t)$ satisfies the algebraic constraint of (7). If Assumption 3 holds, then (7) is an index-0 DAE, meaning that its solution can be obtained by algebraically eliminating the latent variable z to obtain an ODE form. Then, for $t = (k+1)\mathrm{T_d}$, (8) yields

$$x((k+1)\mathrm{T_d}) = e^{\mathrm{T_d}\mathcal{A}(p(k\mathrm{T_d}))}x(k\mathrm{T_d}) + \mathcal{A}^{-1}(p(k\mathrm{T_d}))[e^{\mathrm{T_d}\mathcal{A}(p(k\mathrm{T_d}))} - I]\mathcal{B}(p(k\mathrm{T_d}))u(k\mathrm{T_d}). \tag{9}$$

This solution implies a DT realization of the original system, however as $e^{\mathrm{T_d}\mathcal{A}(p)}$ is not a rational function of $\Delta(p)$, it is not possible to find an exact DT-LFR which describes the state-transition from $(x(k\mathrm{T_d}), u(k\mathrm{T_d}))$ to $x((k+1)\mathrm{T_d})$ defined by (9). One option is to introduce

$$\Delta_\mathrm{d}(k) = \begin{bmatrix} \Delta(p(k\mathtt{T}_\mathrm{d})) & 0 \\ 0 & e^{\mathtt{T}_\mathrm{d}\mathcal{A}(p(k\mathtt{T}_\mathrm{d}))} \end{bmatrix}, \qquad (10)$$

and provide a DT-LFR realization of (9), which might be rather unattractive for controller synthesis due to issues of conservatism.

Now consider the case when Assumption 3 is not satisfied[1]. Then, (7) is a index-1 DAE, meaning that its solution (if it exists) can only be obtained by differentiating (7) once. In general, such solution also has no exact DT-LFR realization.

These conclusions underlines that opposite to the LTI and the LPV-SS cases, no exact DT projection of the dynamics is available in the LFR case under Assumption 4.

B. Approximative approaches

As we have seen, complete discretization of LFRs is rather difficult, thus it is important to develop approximative methods. By looking at the state-equation of (1a) as a pure ODE, numerical approximations of the resulting CT solution can be applied. Then, by using the algebraic constraints in (1a-b), a DT-LFR can be obtained that approximates the original behavior under Assumption 4. In the literature of numerical methods, such an approach is reported to work well for DAE's with index 0 and 1. Using this methodology, the following approximative methods can be derived:

1) Rectangular (Euler's forward) method: Denote the righthand-side of the state-equation in (1a) as

$$f(x,w,u)(t) = Ax(t) + B_1 w(t) + B_2 u(t). \qquad (11)$$

Then,

$$x(t) = x(k\mathtt{T}_\mathrm{d}) + \int_{\tau=k\mathtt{T}_\mathrm{d}}^{t} f(x,w,u)(\tau)\; d\tau, \qquad (12)$$

defines the state-evolution of (1a) in $[k\mathtt{T}_\mathrm{d}, (k+1)\mathtt{T}_\mathrm{d})$. Left-hand rectangular evaluation of (12) gives that

$$x((k+1)\mathtt{T}_\mathrm{d}) = x(k\mathtt{T}_\mathrm{d}) + \mathtt{T}_\mathrm{d} f(x,w,u)(k\mathtt{T}_\mathrm{d}). \qquad (13)$$

Based on this rectangular approach, the DT approximation of $\mathfrak{R}_\mathrm{LFR}(\mathcal{S})$ reads as

$$\mathfrak{R}_\mathrm{LFR}(\mathcal{S},\mathtt{T}_\mathrm{d}) \approx \begin{bmatrix} I+\mathtt{T}_\mathrm{d}A & \mathtt{T}_\mathrm{d}B_1 & \mathtt{T}_\mathrm{d}B_2 \\ C_1 & D_{11} & D_{12} \\ C_2 & D_{21} & D_{22} \end{bmatrix} \qquad (14)$$

with $\Delta_\mathrm{d}(p_\mathrm{d}(k)) = \Delta(p(k\mathtt{T}_\mathrm{d}))$. Note that using first-order Taylor approximation of $e^{\mathtt{T}_\mathrm{d}\mathcal{A}(p(k\mathtt{T}_\mathrm{d}))}$ in the complete solution (9) (which is called the Euler method) results in the same DT-LFR realization as (14). It is also important to highlight that the rectangular approach gives the same solution as the full ZOH setting of Figure 1b with Euler discretization of the LTI part, suggesting very poor performance for this method.

2) Polynomial (Hanselmann) method: It is possible to develop other methods that achieve a better approximation of the complete solution (9) but with increasing complexity. One way leads through the use of higher-order Taylor expansions of the matrix exponential:

$$e^{\mathtt{T}_\mathrm{d}\mathcal{A}(p(k\mathtt{T}_\mathrm{d}))} \approx I + \sum_{l=1}^{n} \tfrac{\mathtt{T}_\mathrm{d}^l}{l!}\mathcal{A}(p(k\mathtt{T}_\mathrm{d})). \qquad (15)$$

Substituting (15) into (9) gives the following DT-LFR for $n=2$:

$$\left[\begin{array}{c:cc:c} \sum_{l=0}^{2}\frac{\mathtt{T}_\mathrm{d}^l}{l!}A^l & \sum_{l=1}^{2}\frac{\mathtt{T}_\mathrm{d}^l}{l!}A^{l-1}B_1 & \frac{\mathtt{T}_\mathrm{d}^2}{2}B_1 & \sum_{l=1}^{n}\frac{\mathtt{T}_\mathrm{d}^l}{l!}A^{l-1}B_2 \\ \hdashline C_1 & D_{11} & 0 & D_{12} \\ C_1 A & C_1 B_1 & D_{11} & C_1 B_2 \\ \hdashline C_2 & D_{21} & 0 & D_{22} \end{array}\right]$$

with $\Delta_\mathrm{d}(p_\mathrm{d}(k)) = \left[\begin{smallmatrix} \Delta(p(k\mathtt{T}_\mathrm{d})) & 0 \\ 0 & \Delta(p(k\mathtt{T}_\mathrm{d})) \end{smallmatrix}\right]$. Note that for $n>2$ it is also possible to derive a general formula however it is not reported here, due to space limitations. Additionally, the above defined method is not equivalent to applying polynomial discretization of the LTI part in the spirit of Figure 1b.

3) Padé's expansion method: A different way of approximating the exponential term in (9), is to use a rational approximation in a form of a Padé (i,j) expansion:

$$e^{\mathtt{T}_\mathrm{d}\mathcal{A}(p)} \approx [T_{ij}(\mathtt{T}_\mathrm{d}\mathcal{A}(p))]^{-1} N_{ij}(\mathtt{T}_\mathrm{d}\mathcal{A}(p)), \qquad (16)$$

where

$$T_{ij}(\mathtt{T}_\mathrm{d}\mathcal{A}(p)) = \sum_{l=0}^{j} \tfrac{(i+j-l)!j!}{(i+j)!l!(j-l)!}\left(-\mathtt{T}_\mathrm{d}\mathcal{A}(p)\right)^l, \qquad (17a)$$

$$N_{ij}(\mathtt{T}_\mathrm{d}\mathcal{A}(p)) = \sum_{l=0}^{i} \tfrac{(i+j-l)!i!}{(i+j)!l!(i-l)!}\left(\mathtt{T}_\mathrm{d}\mathcal{A}(p)\right)^l. \qquad (17b)$$

In general, (16) has a much faster convergence rate than (15). Approximation of matrix exponentials by Padé expansions is also viewed as an attractive approach in the numerical literature [15], [16]. Substituting (16) into (9) gives

$$T_{ij}(\mathtt{T}_\mathrm{d}\mathcal{A}(p(k\mathtt{T}_\mathrm{d})))x((k+1)\mathtt{T}_\mathrm{d}) = N_{ij}(\mathcal{A}(\mathtt{T}_\mathrm{d}p(k\mathtt{T}_\mathrm{d})))x(k\mathtt{T}_\mathrm{d}) + \mathtt{T}_\mathrm{d}\hat{N}_{ij}(\mathtt{T}_\mathrm{d}\mathcal{A}(p(k\mathtt{T}_\mathrm{d})))\mathcal{B}(p(k\mathtt{T}_\mathrm{d}))u(k\mathtt{T}_\mathrm{d}). \qquad (18)$$

where for $i=j$

$$\hat{N}_{ii}(\mathtt{T}_\mathrm{d}\mathcal{A}(p)) = \mathcal{A}(p)^{-1}\big(N_{ii}(\mathtt{T}_\mathrm{d}\mathcal{A}(p)) - T_{ii}(\mathtt{T}_\mathrm{d}\mathcal{A}(p))\big) \qquad (19)$$

As T_{ij}, N_{ij}, and $\hat{N}_{ij}$ are rational functions of $\Delta(p)$, there exists a DT-LFR realization of (18). In the case $i=j=1$, the DT-LFR reads

$$\left[\begin{array}{c:ccc:c} \Psi(I+\frac{\mathtt{T}_\mathrm{d}}{2}A) & \frac{\mathtt{T}_\mathrm{d}}{2}\Psi B_1 & \frac{\mathtt{T}_\mathrm{d}}{2}\Psi B_1 & \frac{\mathtt{T}_\mathrm{d}}{2}\Psi B_1 & \mathtt{T}_\mathrm{d}\Psi B_2 \\ \hdashline \Psi(I+\frac{\mathtt{T}_\mathrm{d}}{2}A) & \frac{\mathtt{T}_\mathrm{d}}{2}\Psi B_1 & \frac{\mathtt{T}_\mathrm{d}}{2}\Psi B_1 & \frac{\mathtt{T}_\mathrm{d}}{2}\Psi B_1 & \mathtt{T}_\mathrm{d}\Psi B_2 \\ C_1 & 0 & D_{11} & 0 & D_{12} \\ 0 & 0 & 0 & D_{11} & D_{12} \\ \hdashline C_2 & 0 & D_{21} & 0 & D_{22} \end{array}\right]$$

with $\Psi = (I - \frac{\mathtt{T}_\mathrm{d}}{2}A)^{-1}$ and

$$\Delta_\mathrm{d}(p_\mathrm{d}(k)) = \left[\begin{smallmatrix} \Delta(p(k\mathtt{T}_\mathrm{d})) & 0 & 0 \\ 0 & \Delta(p(k\mathtt{T}_\mathrm{d})) & 0 \\ 0 & 0 & \Delta(p(k\mathtt{T}_\mathrm{d})) \end{smallmatrix}\right].$$

Again, it is important to note that the above defined method is not equivalent with applying Padé discretization of the LTI part in the spirit of Figure 1b.

4) Trapezoidal (Tustin) method: Another approach to the approximation problem is to use different numerical formulas to approximate the state integral (12). By using a trapezoidal evaluation of (12), we obtain:

$$x((k+1)\mathtt{T}_\mathrm{d}) \approx x(k\mathtt{T}_\mathrm{d}) + \tfrac{\mathtt{T}_\mathrm{d}}{2} f|_{k\mathtt{T}_\mathrm{d}} + \tfrac{\mathtt{T}_\mathrm{d}}{2} f|_{(k+1)\mathtt{T}_\mathrm{d}}. \qquad (20)$$

where $f|_t = f(x,w,u)(t)$. Now by applying a change of variables:

$$\breve{x}_\mathrm{d}(k) = \tfrac{1}{\sqrt{\mathtt{T}_\mathrm{d}}}\left(I - \tfrac{\mathtt{T}_\mathrm{d}}{2}A\right)x(k\mathtt{T}_\mathrm{d}) - \tfrac{\sqrt{\mathtt{T}_\mathrm{d}}}{2}B_1 w(k\mathtt{T}_\mathrm{d}) - \tfrac{\sqrt{\mathtt{T}_\mathrm{d}}}{2}B_2 u(k\mathtt{T}_\mathrm{d}), \qquad (21)$$

and assuming that $I - \frac{\mathtt{T}_\mathrm{d}}{2}A$ is invertible, substitution of (21) into (20) gives the DT-LFR:

[1] Note that invertibility of $I - D_{11}\Delta(\mathtt{p})$ is only a sufficient but not a necessary condition for the well-posedness of LFRs.

$$\left[\begin{array}{ccc}\left(I+\frac{\mathrm{T_d}}{2}A\right)\Psi & \sqrt{\mathrm{T_d}}\Psi B_1 & \sqrt{\mathrm{T_d}}\Psi B_2\\ \sqrt{\mathrm{T_d}}C_1\Psi & \frac{\mathrm{T_d}}{2}C_1\Psi B_1+D_{11} & \frac{\mathrm{T_d}}{2}C_1\Psi B_2+D_{12}\\ \sqrt{\mathrm{T_d}}C_2\Psi & \frac{\mathrm{T_d}}{2}C_2\Psi B_1+D_{21} & \frac{\mathrm{T_d}}{2}C_2\Psi B_2+D_{22}\end{array}\right]$$

with $\Delta_{\mathrm{d}}(p_{\mathrm{d}}(k)) = \Delta(p(k\mathrm{T_d}))$ and $\Psi = (I - \frac{\mathrm{T_d}}{2}A)^{-1}$. It can be shown that the trapezoidal approach gives the same solution as the bilinear method.

5) Multi-step methods: The solution (12) can also be numerically approximated via multi-step formulas like the Runge-Kutta, Adams-Moulton, or the Adams-Bashforth type of approaches [17]. However, in the considered ZOH discretization setting, the sampling rate is fixed and sampled data is only available at past and present sampling instants. Therefore it is complicated to apply methods like the Runge-Kutta or the Adams-Moulton approaches. The family of Adams-Bashforth methods does fulfill these requirements (see [17]). The 3-step version of this numerical approach uses the following approximation of $x((k+1)\mathrm{T_d})$:

$$x(k\mathrm{T_d}) + \frac{\mathrm{T_d}}{12}[5f|_{(k-2)\mathrm{T_d}} - 16f|_{(k-1)\mathrm{T_d}} + 23f|_{k\mathrm{T_d}}]. \quad (22)$$

Then introducing a new state-variable

$$\breve{x}_{\mathrm{d}}(k) = [x^\top(k\mathrm{T_d}), f|^\top_{(k-1)\mathrm{T_d}}, f|^\top_{(k-2)\mathrm{T_d}}]^\top, \quad (23)$$

leads to the DT-LFR:

$$\left[\begin{array}{ccc|c|c} I+\frac{23\mathrm{T_d}}{12}A & -\frac{16\mathrm{T_d}}{12}I & \frac{5\mathrm{T_d}}{12}I & \frac{23\mathrm{T_d}}{12}B_1 & \frac{23\mathrm{T_d}}{12}B_2\\ A & 0 & 0 & B_1 & B_2\\ 0 & I & 0 & 0 & 0\\ \hline C_1 & 0 & 0 & D_{11} & D_{12}\\ \hline C_2 & 0 & 0 & D_{21} & D_{22}\end{array}\right]$$

with $\Delta_{\mathrm{d}}(p_{\mathrm{d}}(k)) = \Delta(p(k\mathrm{T_d}))$.

V. Properties of the approaches

Using a similar line of reasoning as in [12], [13], the discretization error of the introduced approaches can be investigated though their numerical properties. These results together with other properties are summarized in Table I. Based on Table I, all the approximative methods are numerically consistent and convergent, which means that by decreasing $\mathrm{T_d}$ the approximation error of the sampled CT behavior also converges to zero. Furthermore, the order of numerical consistency also indicates the convergence rate of this error. This implies that methods with high convergence rate, like the polynomial and Padé approaches, provide more accurate approximations than the other methods with decreasing $\mathrm{T_d}$. Using the results of the numerical convergence analysis it also becomes possible for each method to derive bounds on $\mathrm{T_d}$ which guarantee a certain discretization error. Furthermore, analyzing the numerical stability of the DT projection, it can be concluded that the preservation of uniform frozen stability of the CT-LFR (stability for all constant trajectories of p) is always guaranteed with the trapezoidal and the Padé approaches. With respect to other methods, analytic bounds $\breve{\mathrm{T}}_{\mathrm{d}}$ of the sampling time can be given for which preservation of the frozen stability is guaranteed.

From the numerical view point, the complete method appears to be attractive as it provides errorless conversion with preservation of the frozen stability. However, the main disadvantage of this approach is that the resulting DT system has no direct LFR realization in terms of the original Δ. By hiding the resulting matrix exponential dependence on p_{d} into Δ_{d}, a DT-LFR can be obtained, however this introduces often too much conservatism if the intended use is DT control design. As in LPV control synthesis mostly low complexity (dimension, type of dependence, structure, etc.) of Δ is preferred (see [2]), therefore both for modeling and controller discretization purposes - beside the preservation of stability - the preservation of the original Δ without repetitions is highly valued. This favors approximative methods that give acceptable performance, but with less repetition of Δ in the new Δ_{d} block. For the rectangular, trapezoidal and the Adams-Bashforth methods, $\Delta_{\mathrm{d}} = \Delta$, making these approaches attractive from this point of view. However, in the Adams-Bashforth case, discretization also results in the order increase of the DT system which requires extra memory storage or more complicated controller design depending on the intended use. If the quality of the DT model has priority, then the trapezoidal, polynomial, and the Padé methods are suggested due to their fast convergence and large stability radius. The Padé (n, n)-method is especially attractive as it merges the good properties of the trapezoidal and polynomial approaches like preservation of stability and fast convergence rate for high n. However the price to be paid is an increased number of repetitions of the Δ block.

VI. Simulation examples

In the following a simple example is presented to visualize/compare the properties of the analyzed discretization methods. Consider the following LFR of a continuous-time SISO LPV system $\mathcal{S}$:

$$\mathfrak{R}_{\mathrm{LFR}}(\mathcal{S}) = \left[\begin{array}{cc|cc|c} 66 & -136 & 1 & 0 & 1\\ 116 & -86 & 0 & 1 & 1\\ \hline -58 & 123 & 0 & 0 & 1\\ -10 & 75 & 0 & 0 & 1\\ \hline 1 & 1 & -0.1 & -0.1 & 0.1\end{array}\right]$$

with $\Delta(p) = \left[\begin{smallmatrix} p & 0\\ 0 & p\end{smallmatrix}\right]$ and $\mathbb{P} = [-1, 1]$. For each constant scheduling trajectory, $p(t) = \mathrm{p}$ for all $t \in \mathbb{R}$, $\mathfrak{R}_{\mathrm{LFR}}(\mathcal{S})$ is equivalent with a stable LTI system, meaning that $\mathcal{S}$ is uniformly frozen stable on $\mathbb{P}$.

Consider $\mathfrak{R}_{\mathrm{LFR}}(\mathcal{S})$ in the exact ZOH setting of Figure 2b with sampling rate $\mathrm{T_d} = 0.02$. By applying the discretization methods of Section IV, approximative DT-LFRs of $\mathcal{S}$ have been calculated. For comparison, the full ZOH approach has also been applied on $\mathfrak{R}_{\mathrm{LFR}}(\mathcal{S})$. To demonstrate the performance of the resulting DT descriptions, the output of the original system and its DT approximations have been simulated on the $[0, 1]$ time interval for zero initial conditions and for 100 different realizations of white u_{d} and p_{d} with uniform distribution $\mathcal{U}(-1, 1)$. For fair comparison, the achieved MSE[2] of the resulting output signals $\hat{y}_{\mathrm{d}}$ has been calculated with respect to the output y of $\mathfrak{R}_{\mathrm{LFR}}(\mathcal{S})$ and presented in Table II. In the simulations, the response of $\mathfrak{R}_{\mathrm{LFR}}(\mathcal{S})$ has been calculated via a 5^{th}-order Runge-Kutta numerical approximation (see [17]) with step size 10^{-8}.

[2] *Mean Square Error*, the expected value of the squared estimation error: $\mathcal{E}\left\{\frac{1}{N}\sum_{k=0}^{N-1}\left(y\left(k\mathrm{T_d}\right) - y_{\mathrm{d}}\left(k\right)\right)^2\right\}$, where $\mathcal{E}$ is the expectation operator.

Property	Complete	Rectangular	n^{th}-polynomial	Trapezoidal	Padé (n,n)	Adams-Bashforth
consistency / convergence	always	1^{st}-order	n^{th}-order	2^{nd}-order	n^{th}-order	3^{rd}-order
preservation of stability / N-stab.	always global	frozen with $\breve{\mathtt{T}}_{\text{d}}$	frozen with $\breve{\mathtt{T}}_{\text{d}}$	always frozen	always frozen	frozen with $\breve{\mathtt{T}}_{\text{d}}$
preservation of instability	+	-	-	+	+	-
Δ_{d}-block complexity	not realizable	$1\times\Delta$	$n\times\Delta$	$1\times\Delta$	$3n\times\Delta$	$1\times\Delta$
system order	preserved	preserved	preserved	preserved	preserved	increased

TABLE I

PROPERTIES OF THE DERIVED DISCRETIZATION METHODS

MSE of y_{d}

$\mathtt{T}_{\text{d}}$	Complete	full ZOH	Rectangular	2^{nd}-polynom.	Trapezoidal	Padé $(1,1)$	Adams-Bash.
$2\cdot10^{-2}$, (50Hz)	$1.2\cdot10^{-8}$	$8.67\cdot10^{-2}$	$(*)$	$(*)$	$1.14\cdot10^{-1}$	$3.37\cdot10^{-1}$	$(*)$
$5\cdot10^{-3}$, (0.2kHz)	$6.7\cdot10^{-9}$	$1.2\cdot10^{-3}$	$(*)$	$2.04\cdot10^{-3}$	$9.67\cdot10^{-4}$	$3.64\cdot10^{-4}$	$1.14\cdot10^{-2}$
10^{-4}, (10kHz)	$5.37\cdot10^{-8}$	$5.37\cdot10^{-8}$	$2.19\cdot10^{-7}$	$5.37\cdot10^{-8}$	$9.77\cdot10^{-8}$	$5.37\cdot10^{-8}$	$3.15\cdot10^{-7}$

TABLE II

DISCRETIZATION ERROR OF $\mathcal{S}$, GIVEN IN TERMS OF THE ACHIEVED AVERAGE MSE FOR 100 SIMULATIONS. $^{(*)}$ INDICATES UNSTABLE PROJECTION TO THE DISCRETE DOMAIN.

Thus, the switching effect of the ZOH actuation does not show up in the calculated response.

From the results of Table II it is immediate that, except for the rectangular, polynomial and the Adams-Bashforth methods, all approximations converge. As expected, the error of the complete method is extremely small and the trapezoidal with the Padé $(1,1)$ method give a moderate, but acceptable performance. Surprisingly, the full ZOH approach also gives a stable projection with an acceptable error. This underlines that the full ZOH approach can provide effective discretization of LFRs in some cases. However, its weakness is its unpredictable nature.

As a next step, discretizations of $\mathfrak{R}_{\text{LFR}}(\mathcal{S})$ with $\mathtt{T}_{\text{d}} = 0.005$, the half of the stability bound $\breve{\mathtt{T}}_{\text{d}}$ forthe polynomial method, are calculated. The simulation results for this case are given in the second row of Table II. The rectangular method again results in an unstable projection, while the Adams-Bashforth method seems to be stable, but its numerical stability is not guaranteed for all trajectories of p_{d}. The trapezoidal and the Padé method also improve significantly in performance, however the Padé seems to outperform the trapezoidal method due to its faster convergence rate.

As a next step, discretizations of $\mathfrak{R}_{\text{LFR}}(\mathcal{S})$ with $\mathtt{T}_{\text{d}} = 10^{-4}$, the half of the $\breve{\mathtt{T}}_{\text{d}}$ bound for the rectangular method, are calculated and simulated. The results are given in the third row of Table II. Finally, the rectangular method converges and also the approximation capabilities of the other methods reach the numerical step-size (10^{-8}) of the continuous-time simulation.

VII. CONCLUSIONS

In this paper, discretization approaches of Linear Fractional Representations of LPV systems were introduced using an exact ZOH setting where the variation of the state coupled by the scheduling dependent Δ-block is not restricted inside the sampling interval. This provides an advantage over existing methods to reduce the introduced discretization error. The developed approaches were analyzed in terms of applicability and numerical properties, giving an overview of which methods are attractive depending on the aim and achievable sampling time of the discretization. An illustrative example was provided to give insight into the derived methods and their properties.

REFERENCES

[1] A. Packard and G. Becker, "Quadratic stabilization of parametrically-dependent linear system using parametrically-dependent linear, dynamic feedback," *Advances in Robust and Nonlinear Control Systems*, vol. DSC, no. 43, pp. 29–36, 1992.

[2] C. W. Scherer, "Mixed $\mathcal{H}_2/\mathcal{H}_\infty$ control for time-varying and linear parametrically-varying systems," *Int. Journal of Robust and Nonlinear Control*, vol. 6, no. 9-10, pp. 929–952, 1996.

[3] K. Zhou and J. C. Doyle, *Essentials of Robust Control*. Prentice-Hall, 1998.

[4] P. Apkarian and P. Gahinet, "A convex characterization of gain-scheduled $\mathcal{H}_\infty$ controllers," *IEEE Trans. on Automatic Control*, vol. 40, no. 5, pp. 853–864, 1995.

[5] A. Packard, "Gain scheduling via linear fractional transformations," *System Control Letters*, vol. 22, no. 2, pp. 79–92, 1994.

[6] J. Kim, D. G. Bates, and I. Postletwaite, "Robustness analysis of linear periodic time-varying systems subject to structured uncertainty," *Systems and Control Letters*, vol. 55, pp. 719–725, 2006.

[7] L. Ma and P. Iglesias, "Robustness analysis of a self-oscillating molecular network in a dictostelium discoideum," in *Proc. of the 41th IEEE Conf. on Decision and Control*, Las Vegas, Nevada, USA, Dec. 2002, pp. 2538–2543.

[8] D. Peaucelle, C. Farges, and D. Arzelier, "Robust LFR-based technique for stability analysis of limit cycles," in *Proc. of the IFAC Symposium ALCOSP'07/PSYCO'07*, St. Petersburg, Russia, Aug. 2007.

[9] N. Imbert, "Robustness analysis of a launcher attitude controller via μ-analysis," in *Proc. of the 15th IFAC Symposium on Automatic Control in Aerospace*, Bologne, Italy, Sept. 2001, pp. 429–434.

[10] P. C. Pellanda, P. Apkarian, and H. D. Tuan, "Missile autopilot design via a multi-channel LFT/LPV control method," *Int. Journal of Robust and Nonlinear Control*, vol. 12, pp. 1–20, 2002.

[11] G. Ferreres, "Reduction of dynamic LFT systems with LTI model uncertainties," *Int. Journal of Robust and Nonlinear Control*, vol. 14, pp. 307–323, 2004.

[12] R. Tóth, F. Felici, P. S. C. Heuberger, and P. M. J. Van den Hof, "Crucial aspects of zero-order-hold LPV state-space system discretization," in *Proc. of the 17th IFAC World Congress*, Seoul, Korea, July 2008, pp. 3246–3251.

[13] R. Tóth, "Modeling and identification of linear parameter-varying systems, an orthonormal basis function approach," Ph.D. dissertation, Delft University of Technology, (http://www.dcsc.tudelft.nl/~pvandenhof/Paperfiles/Toth_PhDThesis_2008.pdf), 2008.

[14] K. J. Åström and B. Wittenmark, *Computer controlled systems*. Prentice-Hall, 1990.

[15] C. B. Moler and C. F. Van Loan, “Nineteen dubious ways to compute the exponential of a matrix, twenty-five years later,” *SIAM Review*, vol. 45, no. 1, pp. 3–49, 2003.

[16] B. N. Datta, *Numerical methods for linear control systems*. Elsevier, 2004.

[17] K. E. Atkinson, *An Introduction to Numerical Analysis*. John Wiley and Sons, 1989.